Journal of Sound and Vibration (2002) **250**(2), 339–349
doi:10.1006/jsvi.2001.3918, available online at http://www.idealibrary.com on IDEAL®

NORMAL MODES OF A NON-LINEAR CLAMPED–CLAMPED BEAM

W. C. Xie, H. P. Lee and S. P. Lim

Department of Mechanical Engineering, National University of Singapore, 9 *Engineering Drive* 1, *Singapore* 117576, *Singapore. E-mail*: *mpeleehp@nus.edu.sg*

(*Received* 11 *April* 2001, *and in final form* 7 *August* 2001)

Non-linear modal analysis approach based on invariant manifold method proposed earlier by Shaw and Pierre (*Journal of Sound and Vibration* **164**, 85–124) is utilized here to obtain the non-linear normal modes of a clamped–clamped beam for large amplitude displacements. The results obtained for the fundamental normal mode are compared with the corresponding reported experimental and theoretical studies. The effects of modal coupling are examined in greater detail. The limitation of the present method for analyzing non-linear behavior is highlighted.

1. INTRODUCTION

Clamped–clamped structures at large amplitude displacements are frequently encountered in many engineering applications. The problem of computing the normal modes of such a non-linear continuous system has received much attention recently. It is interesting to know the non-linear behavior of thin beams with axial restraint at the ends. The non-linear normal modes can be used to determine the near-resonance response of beams.

MacDonald [1] found that a uniform beam with hinged ends subjected to a concentrated force at its mid-point, with arbitrary initial conditions, exhibited a dynamic coupling of its modes of vibrations. Smith *et al.* [2] experimentally studied the non-linear behavior of a clamped–clamped thin aluminum strip under sinusoidal pressure excitation and showed that the fundamental mode shape was much flatter at mid-span and had high curvature at the ends at large amplitude vibration. Tseng and Dugundji [3] investigated the non-linear vibrations of a clamped–clamped beam excited by sinusoidal motion of its supports in a direction normal to its span, and indicated that, for large amplitude vibration, the general solution involved the forcing frequency component as well as the superharmonic and subharmonic components. Busby and Weingarten [4] derived an approximate solution for the non-linear differential equation of clamped–clamped beams, and indicated that the phenomenon of coupled resonance would occur if the non-linear stiffness terms were large. Bennouna and White [5] experimentally and theoretically investigated the fundamental mode shape of a clamped–clamped beam. They suggested that the amplitude-dependent, normalized fundamental mode shape had a high relative value near the clamped ends at large amplitude deflection and the bending strain would increase due to the changes in mode shape as well as the axial strain. Qaisi [6, 7] employed a power-series approach for the analysis of non-linear vibration of beams with restrained end supports and resting on a non-linear foundation. Ghanbari and Dunne [8] experimentally examined the non-linear damping model for large amplitude random vibration of a clamped–clamped beam.

Modal analysis first emerged around 1940, as a reliable analysis tool that provides an understanding of structural characteristics, operating conditions and performance criteria that enables designing for optimal behavior or solving structural dynamic problems in existing designs. In linear systems, one of the most important properties is the superposition principle. That is, a general motion can be written as a linear combination of the normal modes. However, it does not hold for a non-linear system, but it is still possible to define non-linear normal modes. Using a geometric method, a concept of non-linear normal modes, following that of the linear ones, was first introduced by Rosenberg [9]. A basic property of the linear system as well as the non-linear system is that motion consisting of a single mode at any instant will consist only of the mode at all times, moreover, all the co-ordinates cross their equilibrium positions simultaneously and also achieve their maximum values at the same time. The concept of non-linear normal modes has been developed by many subsequent efforts. It has given significant insight into the dynamics of non-linear systems and has provided a systematic method for modal reduction. Szemplinska-Stupnicka [10] applied the simple harmonic balance approach to attain the non-linear modes of a multi-degrees-of-freedom system. In terms of two-dimensional invariant manifold, Shaw and Pierre [11, 12] proposed a methodology to construct normal modes for non-linear continuous systems. Based on the method of multiple scales, Nayfeh and Nayfeh [13] and Nayfeh *et al.* [14] obtained results in agreement with those from the invariant manifold method.

In this present work, we construct the non-linear normal modes of clamped–clamped beams. A combination of invariant manifold method and Galerkin procedure proposed earlier by Shaw and Pierre [11, 12] has been used. The effects of non-linearities can be easily tracked to different orders of linear modes. The non-linear normal modes are obtained as a combination of certain linear normal modes. The contributions of different linear modes are easily detected. The numerical results show good agreement with available experimental results. Moreover, how far the characteristics of the normal mode corresponding to large amplitude vibration deviate from those of the linear theory are also of interest to us. The effects of modal coupling are examined. The limitation of the present method in analyzing non-linear behavior is highlighted.

2. FORMULATION

The problem considered is the free vibration of Euler–Bernoulli clamped–clamped beam under large amplitude deflection. Compared to linear beams, the tension induced in axially constrained beams from stretching must be considered, especially under large deflection. The governing non-linear partial differential equation [15] is

$$\rho A \frac{\partial^2 w^*(x^*, t^*)}{\partial t^{*^2}} + EI \frac{\partial^2 w^*(x^*, t^*)}{\partial x^{*^4}} - \frac{EA}{2L} \frac{\partial^2 w^*}{\partial x^{*^2}} \int_0^L \left(\frac{\partial w^*(x^*, t^*)}{\partial t^*} \right)^2 \mathrm{d}x^* = 0 \qquad (1)$$

subject to the boundary conditions:

$$\partial w^*/\partial x^* = w^* = 0 \quad \text{at } x^* = 0 \quad \text{and} \quad x^* = L^*, \qquad (2)$$

where $w^*(x^*, t^*)$ is the transverse displacement at position x^* in the domain $(0, L)$ and time t^*, EI is the flexural rigidity, ρ and A are the beam mass density and cross-sectional area, respectively, and L is the beam length. The introduction of the non-dimensional quantities

$$x = \frac{x^*}{L}, \qquad t = \frac{t^*}{L^2}\sqrt{\frac{EI}{\rho A}}, \qquad w = \frac{w^*}{D}, \qquad (3)$$

into equations (1) and (2) results in the following non-dimensional form:

$$\ddot{w} + w^{iv} = \alpha w'' \int_0^1 (w')^2 \, dx \tag{4}$$

and associated boundary conditions

$$w = w' = 0 \quad \text{at } x = 0 \text{ and } 1, \tag{5}$$

where D is a characteristic transverse displacement (either L or h), $\alpha = D^2 A/2I$, the overdot and prime represent partial derivative with respect to time t and the distance along the beam x respectively. The equation of motion is of second order in time derivatives and of arbitrary order in spatial derivatives. We rewrite equation (4) in the form

$$\ddot{w} + L[w(x, t)] + N[w(x, t)] = 0, \tag{6}$$

where L and N are linear and non-linear, self-adjoint spatial operator.

Shaw and Pierre [11, 12] presented a methodology to treat this kind of non-conservative and/or gyroscopic continuous systems. They used a set of two-dimensional invariant manifolds in phase space that represent normal mode motions for non-linear system, and then provided the equations of motion that dictate the dynamics on these manifolds. The manifold passes through a stable equilibrium point $(w, \dot{w})$ and is tangential to the eigenspaces of the associated linearized system at that point. They described the response of systems by the response of a single point on the structure through the amplitude-dependent mode shape

$$w(x, t) = W(w_0(t), \dot{w}(t), x, x_0), \quad \dot{w}(x, t) = \dot{W}(w_0(t), \dot{w}(t), x, x_0). \tag{7}$$

The normal mode manifolds are obtained through the asymptotic expansion of $w(x, t)$ and $\dot{w}(x, t)$, which correspond to a non-linear separation of variables. However, the choice of the reference point x_0 makes the method cumbersome. Boivin *et al.* [16] modified the approach by first applying the Galerkin procedure, with normal modes as trial functions, to discretize the systems and obtain a sequence of ordinary differential equations. This approach avoids several complications and is fairly straightforward to implement.

Nayfeh and Nayfeh [13] and Nayfeh *et al.* [14] applied the method of multiple scales directly to the governing partial differential equation and boundary conditions to obtain an approximation to the non-linear modes and natural frequencies, $w(x, t)$ is first expanded in a first order uniform series of the form

$$w(x, t; \varepsilon) = w_0(x, T_0, T_1) + \varepsilon w_1(x, T_0, T_1) + \cdots, \tag{8}$$

where $T_0 = t$ and εt are fast scale and slow scale at one of the natural frequencies. From an example of a cantilever beam, they got results which were equivalent to those obtained from invariant manifold techniques.

Based on the modified Shaw and Pierre's method [16], the computation of solution of the governing equation (6) and boundary conditions (5) begins by discretizing the continuous system using series of linear eigenfunctions of the form

$$w(x, t) = \sum_{i=1}^{\infty} \phi_i(x) q_i(t), \tag{9}$$

where $q_i(t)$ are time-dependent generalized modal co-ordinates and $\phi_i(x)$ are the linear mode shapes corresponding to the linear problem

$$\phi_i(x) = [(\cosh \lambda_i x - \cos \lambda_i x) + \beta_i (\sinh \lambda_i x - \sin \lambda_i x)], \tag{10}$$

where

$$\beta_i = \frac{\cos\lambda_i - \cosh\lambda_i}{\sinh\lambda_i - \sin\lambda_i}. \tag{11}$$

The eigenvalue parameters λ_i are the positive roots of frequency equation

$$\cos\lambda_i \cosh\lambda_i = 1. \tag{12}$$

Equation (12) admits a countable infinite number of solutions for λ_i, and for each value of λ_i, there are a corresponding mode shape $\phi_i(x)$ and a natural frequency ω_i, given by λ_i^2. For the linear system, the linear normal modes satisfy

$$\langle \phi_i(x), \phi_j(x) \rangle = \delta_{ij}, \tag{13}$$

$$\langle L[\phi_i(x)], \phi_j(x) \rangle = \omega_i^2\, \delta_{ij}, \tag{14}$$

where $\langle f, g \rangle$ denotes the usual inner product defined as $\langle f, g \rangle = \int_\Omega f(x) g(x)\, \mathrm{d}x$ and δ_{in} is the Kronecker delta, defined by $\delta_{in} = 0$ if $i \neq n$ and $\delta_{in} = 1$ if $i = n$.

On substituting equation (9) into equation (6) and taking the inner product of the resulting equation with $\phi_j(x)$, equation (6) becomes a set of non-linear ordinary differential equations uncoupled at the linear order and coupled via the non-linear term

$$\ddot{q}_j + \omega_j^2 q_j + N_j(q) = 0 \quad \text{for } j = 1, 2, 3 \ldots, \tag{15}$$

where

$$N_j(q) = \left\langle \phi_k(x), N\left(\sum_{n=1}^{\infty} \phi_i(x) q_i(t)\right)\right\rangle. \tag{16}$$

Equation (15) is first rewritten in two first order forms as

$$\dot{q}_j = p_j, \qquad \dot{p}_j = -\,\omega_j^2 q_j - N_j(q). \tag{17a, b}$$

Then, to construct the two-dimensional manifold that reduces to the kth linear mode as the non-linearity vanishes, the jth mode is related to the kth mode as follows:

$$q_j(t) = Q_{jk}(q_k, p_k), \qquad p_j(t) = P_{jk}(q_k, p_k). \tag{18}$$

Because the manifold is tangential to the linear eigenspaces of the kth mode at the equilibrium point, $(Q_{jk}(0, 0), P_{jk}(0, 0)) = (0, 0)$ is the equilibrium configuration of the system. Q_{jk} and P_{jk} are at least quadratic functions of q_k, p_k. For the case of cubic geometric non-linearity as indicated in equation (1), we can express the non-linearity as

$$N_j(q) = g_{jk}\, q_k^3, \tag{19}$$

where g_{jk} is given by

$$g_{jk} = \left\langle \phi_j(x),\ -\alpha\phi_k'' \int_0^1 \phi_k'^2\, \mathrm{d}x \right\rangle. \tag{20}$$

According to the form of the non-linearity in equation (15), Q_{jk} and P_{jk} are given in the form

$$Q_{jk} = h_{1jk}\, q_k^3 + h_{2jk}\, q_k\, p_k^2,$$

$$P_{jk} = h_{3jk}\, q_k^2 p_k + h_{4jk}\, p_k^3. \tag{21}$$

Substituting equations (18)–(21) into equations (17a) and (17b) and equating the coefficients of q_k^3, $q_k p_k^2$, $q_k^2 p_k$ and p_k^3 yield the following four equations to be solved:

$$\begin{aligned} 3h_{1jk} - 2h_{2jk}\omega_k^2 - h_3 &= 0, \\ h_{2jk} - h_{4jk} &= 0, \\ 2h_{3jk} - 3h_{4jk}\omega_k^2 + h_{2jk}\omega_j^2 &= 0, \\ h_{1jk}\omega_j^2 - h_{3jk}\omega_k^2 &= -g_{jk}. \end{aligned} \tag{22}$$

Solving the equations give

$$h_{1jk} = \frac{g_{jk}(7\omega_k^2 - \omega_j^2)}{(9\omega_k^2 - \omega_j^2)(\omega_k^2 - \omega_j^2)}, \qquad h_{2jk} = h_{4jk} = \frac{6g_{jk}}{(9\omega_k^2 - \omega_j^2)(\omega_k^2 - \omega_j^2)}$$

$$h_{3jk} = \frac{3g_{jk}(3\omega_k^2 - \omega_j^2)}{(9\omega_k^2 - \omega_j^2)(\omega_k^2 - \omega_j^2)} \quad \text{for } j \neq k. \tag{23}$$

The kth non-linear mode is determined in third order non-linearity by

$$w_k(x, t) = \phi_k(x)\, q_k(t) + \sum_{j \neq k} \phi_j(x)[h_{1jk}q_k^3(t) + h_{2jk}q_k q_k^2(t)], \tag{24}$$

where q_k is governed by

$$\ddot{q}_k + \omega_k^2 q_k + g_{kk}\, q_k^3 = 0. \tag{25}$$

The exact mathematical solution can be given in terms of the Jacobean elliptic function C_n of the form [17–19]

$$q_k(t) = a_k\, C_n(\gamma t, k), \quad \gamma = \omega^2 \sqrt{1 + \frac{g_{kk}}{\omega_k^2} a_k^2}, \quad k^2 = \frac{g_{kk}}{2\gamma^2} a_k^2, \tag{26a–c}$$

where k is the modulus of the elliptic function and γ is the circular frequency. The elliptic function C_n is periodic with a period of $4K(k)$, where K is the complete elliptic integral of the first kind. The period on t of $q_k(t)$ is

$$T = \frac{4}{\gamma} K(k) \quad \text{with } K(k) = \int_0^{\pi/2} \frac{\mathrm{d}\theta}{\sqrt{1 - k^2 \sin^2\theta}}. \tag{27}$$

Nayfeh [20] applied the method of normal forms to obtain an approximate solution for the dynamics of the kth non-linear mode of the form

$$q_k(t) = a_k \cos(\omega_{Nk}t + \beta_{k0}) + \frac{g_{kk}}{32\omega_k^2} a_k^3 \cos(3\omega_{Nk}t + 3\beta_{k0}) + \cdots, \tag{28}$$

where a_k and β_{k0} are constants depending on the initial conditions. The non-linear natural frequency of the kth mode is

$$\omega_{Nk} = \omega_k + \frac{3g_{kk}a_k^2}{8\omega_k} + \cdots. \tag{29}$$

Equation (24) represents a form of non-linear separation of variables which recovers the linear dynamics when non-linearities are neglected and systematically produced the non-linear corrections to the normal modes. It is a direct consequence of the definition of the non-linear modes, which are tangential to their linear counterpart at the system's equilibrium.

The amplitude dependence of the non-linear mode shapes and frequencies is clearly exhibited by equations (24) and (28). Note that whenever $q_k(t_0) = 0$, $w_k(x, t_0) = 0$ for all x at that instant of time. When $p_k(t^*) = 0$, $q_k(t^*) = q_k^*$ is maximum and $w_k(x, t_0)$ is extreme for all x. This implies that the beam motion in a given non-linear normal mode is synchronous. Normal mode shapes are most easily observed at peak displacement, i.e., when $p_k(t) = 0$. Thus, the mode shape $W_k(x)$ is defined by

$$W_k(x) = \phi_k(x) q_k^* + \sum_{j \neq k} \phi_j(x) h_{1jk} q_k^{*3}. \tag{30}$$

As seen from equation (30), the non-linear normal mode shapes as well as the contributions from non-resonance modes are amplitude-dependent. It should be noted that the property of synchronous holds for cubic non-linearity as in this case. For systems with a combination of quadratic and cubic non-linearity, the response of various points would not necessarily have zero deflection at the same time.

3. RESULTS AND DISCUSSION

As shown in equation (15), g_{jk} are dynamic coefficients that combine the dynamics of different modes via the corresponding non-linear item, h_{1jk} are coefficients that include the contributions from other modes in cubic order (see equation (30)). It was found that changes of generalized parameter caused the change in mode shapes at large amplitude deflection. Both g_{jk} and h_{1jk} are proportional to α, which is a material parameter and is related to the dimension of the beam. It implies that the more slender the beam, the stronger the non-linearity under large amplitude vibration. The generalized parameters in the linear normal modes are not applicable to the non-linear normal modes. The non-dimensional parameters $g_{jk}/-\alpha = \int_0^1 \phi_j(x)\phi_k'' \int_0^1 (\phi_k')^2 \, \mathrm{d}x \, \mathrm{d}x$ and h_{1jk}/α are listed in Tables 1 and 2, respectively, for the first six modes.

Linear normal modes are orthogonal to one another, and it does not hold for non-linear beams. However, the property of orthogonality still exists between the odd and even order

TABLE 1

Non-dimensional non-linear dynamic coefficients

$-g_{jk}/-\alpha$	$k = 1$	2	3	4	5	6
$j = 1$	− 151·354	0	962·422	0	2010·5	0
2	0	− 2120·6	0	2939·1	0	5700
3	119·714	0	− 9782·16	0	6428·3	0
4	0	788·79	0	− 29 440	0	8823
5	93·6898	0	2408·32	0	− 7e4	0
6	0	699·71	0	4024·94	0	11 521
7	75·1449	0	1704·94	0	7529·9	0
8	0	453·71	0	3935·13	0	12 601
9	46·7487	0	1546·84	0	7516·2	0
10	0	394·77	0	3688·79	0	12 739
11	10	0	1000	0	7000	0
12	0	300	0	3000	0	10 000

TABLE 2

Non-dimensional coefficients

h_{1jk}/α	$k = 1$	2	3	4	5	6
$j = 1$	/	0	− 5·2967e − 2	0	− 1·7639e − 2	0
2	0	/	0	− 6·3059e − 2	0	−2·6048e −2
3	9·3196e − 3	5·0893e − 2	/	0	− 6·6740e − 2	0
4	0	—	0	/	0	−5·0855e −2
5	1·0695e − 3	0	1·0047e − 2	0	/	0
6	0	4·3382e − 3	0	1·7117e − 2	0	/
7	2·4501e − 4	0	6·7683e − 3 0		2·1968e − 2	0
8	0	9·1343e − 4	0	1·2902e − 2	0	2·5264e − 2
9	5·9034e − 5	0	2·0740e − 3	0	− 2·0515e − 1	0
10	0	3·3670e − 4	0	3·5367e − 3	0	1·0977e − 3
11	2·3499e − 5	0	6·0305e − 4 0		5·1929e − 3	0
12	0	1·2676e − 4	0	1·3338e − 3	0	6·4767e − 3

TABLE 3

Numerical and experimental analyses of the fundamental mode shape at $D/h = 2{\cdot}1$

x	W^*1	W^*2	W^*3
0	0	0	0
0·025	0·00846	0·0338	0·018776
0·05	0·03249	0·075	0·067414
0·075	0·07004	0·1339	0·135423
0·1	0·11907	0·2103	0·21478
0·125	0·17757	0·278	0·300358
0·15	0·24352	0·3449	0·389005
0·175	0·31497	0·4141	0·478003
0·2	0·39001	0·4832	0·564069
0·225	0·46677	0·5542	0·643604
0·25	0·54348	0·6252	0·713863
0·275	0·61846	0·6834	0·774036
0·3	0·69011	0·7456	0·825278
0·325	0·75699	0·8	0·86956
0·35	0·81776	0·8453	0·908159
0·375	0·87125	0·8817	0·940865
0·4	0·91645	0·9181	0·966464
0·425	0·95349	0·9563	0·984062
0·45	0·97873	0·97873	0·99419
0·475	0·99466	0·99466	0·998782
0·5	1	1	1

non-linear normal modes. It can be demonstrated from equation (30) and Tables 1 and 2 that odd order non-linear modes comprise a combination of odd order linear normal modes, and even order non-linear modes consist of a combination of even order linear modes. No mode coupling effects exist between odd order normal modes and even order normal modes. This is in agreement with the results obtained by Chakraborty *et al.* [21].

Bennouna and White [5] examined experimentally the fundamental mode shape of a slender clamped–clamped beam of dimensions $2 \times 20 \times 610$ mm made of aluminum DTD

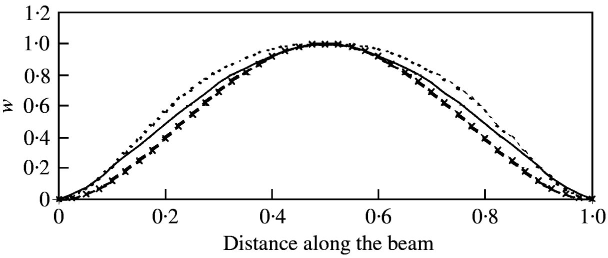

Figure 1. Comparison of the fundamental mode shape: – – × – –, linear; ——, experimental; – – –, invariant manifold.

TABLE 4

Modal coupling effects

x	$D4$	$D6$	$D8$	$D10$	$D12$	DL	DM
0·000	0·00000	0·00000	0·00000	0·00000	0·00000	0·00000	0·00000
0·025	0·01547	0·01651	0·01724	0·01743	0·01878	0·00846	0·03380
0·050	0·05796	0·06125	0·06355	0·06404	0·06741	0·03249	0·07500
0·075	0·12160	0·12713	0·13098	0·13155	0·13542	0·07004	0·13390
0·100	0·20067	0·20737	0·21209	0·21236	0·21478	0·11907	0·21030
0·125	0·28971	0·29575	0·30039	0·30006	0·30036	0·17757	0·27800
0·150	0·38366	0·38686	0·39056	0·38958	0·38900	0·24352	0·34490
0·175	0·47802	0·47633	0·47864	0·47723	0·47800	0·31497	0·41410
0·200	0·56899	0·56086	0·56191	0·56047	0·56407	0·39001	0·48320
0·225	0·65349	0·63828	0·63871	0·63762	0·64360	0·46677	0·55420
0·250	0·72932	0·70740	0·70816	0·70757	0·71386	0·54348	0·62520
0·275	0·79508	0·76788	0·76984	0·76963	0·77403	0·61846	0·68340
0·300	0·85018	0·81995	0·82362	0·82344	0·82527	0·69011	0·74560
0·325	0·89473	0·86418	0·86952	0·86900	0·86956	0·75699	0·80000
0·350	0·92942	0·90128	0·90767	0·90663	0·90816	0·81776	0·84530
0·375	0·95536	0·93190	0·93837	0·93691	0·94086	0·87125	0·88170
0·400	0·97391	0·95656	0·96208	0·96053	0·96646	0·91645	0·91810
0·425	0·98467	0·97559	0·97943	0·97818	0·98406	0·95349	0·95630
0·450	0·99437	0·98915	0·99112	0·99041	0·99419	0·97873	0·97873
0·475	0·99865	0·99729	0·99782	0·99762	0·99878	0·99466	0·99466
0·500	1·00000	1·00000	1·00000	1·00000	1·00000	1·00000	1·00000

S070 at large deflection. Here, the experimentally investigated fundamental mode shape of the beam at $W_1/h = 2{\cdot}1$ are compared with the analytical results from the invariant manifold method, where W_1/h is the maximum amplitude at mid-point/beam thickness. In Table 3, W^*1 is the theoretical normalized fundamental mode shape of the beam (linear), W^*2 is the measured normalized mode shape, and W^*3 is the normalized mode shape calculated from invariant manifold method. The peak amplitude along half of the beam at intervals of 0·0251 was used for the mode shape estimates, and symmetry is assumed. The comparison is visualized in Figure 3. Although the numerical values are different, both the numerical and experimental mode captures the same features of the non-linear mode and exhibits the same trends. The result suggests that for clamped–clamped beams, the linear modes are different from the non-linear modes, that is, at large amplitude deflection. The influence of non-linearities is clearly illustrated in Figure 1. An attempt was made to increase the accuracy by increasing the number of normal modes involved. However, for the

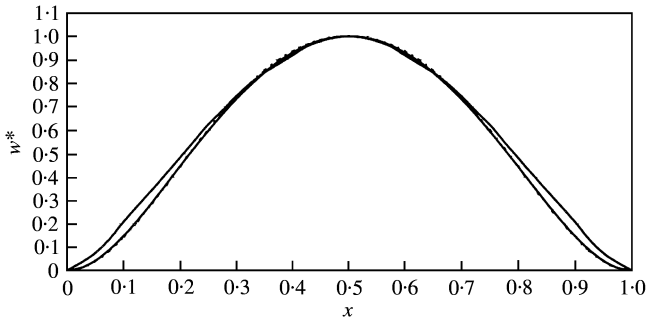

Figure 2. Convergence of model coupling for the fundamental mode shape: ——, experimental; – – –, up to four terms; ——, up to six terms.

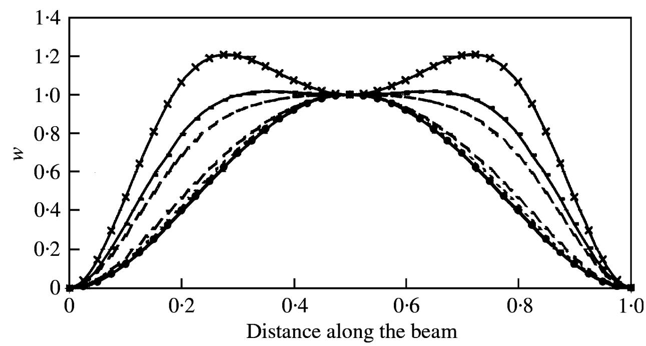

Figure 3. Comparison of the first normal mode shape as the amplitude increases: ——, linear; —●—, $Y/h = 0{\cdot}5$; – – –, $Y/h = 1{\cdot}0$; —-—-, $Y/h = 1{\cdot}5$; – – –, $Y/h = 2{\cdot}5$; ——, $Y/h = 2{\cdot}7$; —×—, $Y/h = 2{\cdot}9$.

fundamental non-linear mode, the third linear modes have the most significant effect on the fundamental non-linear mode. The higher the modes are, the less the effects are. These are shown in Table 4 and Figure 2, where DN are numerical results from the current method, N denotes the linear modes used for approximation, and DL represents the linear results and those from the experiment respectively.

The contribution of other modes is to be amplitude dependent, or dependent on the maximum amplitude. The peak amplitudes have a significant influence on the combinational effects of the different normal modes. The influence of various linear modes on the non-linear modes can be visualized easily. The fundamental non-linear normal mode and the second non-linear mode depicted in Figures 3 and 4 illustrate the amplitude-dependent shape as the amplitude increases. From Figures 3 and 4, we can see that, as the amplitude increases, at the mid-span of the beam, both the fundamental and second mode shapes have higher curvature at points near the two clamped ends. For the first mode shape, it also turns flatter at the mid-span of the beam at large amplitude. The second non-linear mode shape deviates from the linear mode shape significantly. However, when the amplitude is small, i.e., less than h, the non-linear mode approaches the linear mode. Thus, the non-linearity induced by the tension in clamped–clamped beam is negligible at small amplitude vibration. It is possible to obtain quite accurate results by neglecting the non-linear coupling terms and considering each mode individually for response prediction. It was also observed that lower linear modes contribute negative effects to higher non-linear modes, while the contribution from higher linear modes to the lower non-linear modes are

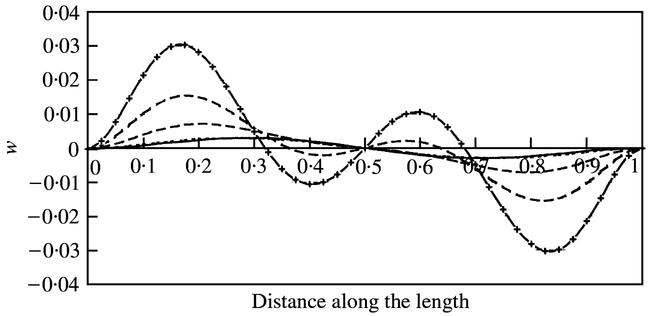

Figure 4. Comparison of the second mode shape as the amplitude increases: ——, linear; - - -, non-linear; $Y/L = 0{\cdot}002$; — - - —, non-linear, $Y/L = 0{\cdot}004$; – – –, non-linear, $Y/L = 0{\cdot}006$; —+—, non-linear, $Y/h = 0{\cdot}008$.

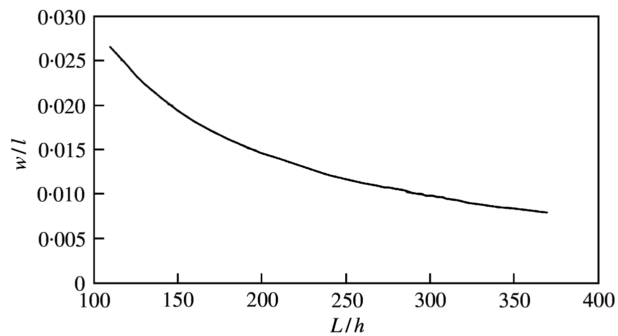

Figure 5. Maximum amplitude deflection at mid-point of the beam.

positive. When the normalized beam amplitudes $> 1{\cdot}5$, at least two modes are considered needed for accurate response prediction.

As seen in Figure 3, when the amplitude/thickness ratio is 2·7, the fundamental non-linear mode shape no longer resembles the shape as in those of lower ratios. This is mainly from the modal coupling effects, i.e., the higher linear modes have a stronger effect on the composition of the fundamental non-linear mode shape. The current method is based on the assumption that the motion of each co-ordinate will reach its maximum, either in positive or in negative direction, at exactly the same time. This is only true if the eigenvector elements (mode shapes) are real quantities (positive or negative). However, when the amplitude/thickness ratio reaches 3·0, equations (24) and (30) give a complex value, and the non-linear normal modes are not synchronous for a beam of such strong non-linearity. Therefore, the invariant manifold method is not suitable for clamped–clamped beam of such a case. Figure 5 gives the restriction for different ratios of length/thickness.

4. CONCLUSION

Normal modes for a clamped–clamped beam at large amplitude displacement have been examined by using non-linear normal modes and invariant manifold method developed earlier by several researchers [9, 11–14, 16]. The Galerkin procedure is applied to decouple the non-linear partial differential governing equations. The individual linear normal modes are shown to have an effect on the non-linear modes at large amplitudes. A comparison between the measurement and current method exhibits the same trends for the fundamental mode. The orthogonality between the odd and even order non-linear normal modes is verified. Higher curvatures with the increase of the amplitudes are found near the clamped ends. When the amplitude/thickness ratio reaches 3·0 and strong non-linearity emerges, the current method is not suitable for this system. The non-linear normal modes are useful for model reduction and in determining the near-resonance response of the clamped–clamped beams.

REFERENCES

1. P. H. MacDonald 1995 *Journal of Applied Mechanics* **22**, 573–578. Nonlinear dynamic coupling in a beam vibration.
2. P. W. Smith, C. I. Malme and C. M. Gogos 1961 *Journal of the Acoustical Society of America* **33**, 1476–1480. Nonlinear response of a simple clamped panel.
3. W. Y. Tseng and Dugundji 1970 *Journal of Applied Mechanics* **37**, 292–297. Nonlinear vibrations of a beam under harmonic excitation.
4. H. R. Busby and V. I. Weingarten 1972 *International Journal of Nonlinear Mechanics* **7**, 289–303. Nonlinear response of a beam to period loading.
5. M. M. Bennouna and R. G. White 1984 *Journal of Sound and Vibration* **96**, 309–331. The effects of large vibration amplitudes on the fundamental mode shape of a clamped–clamped uniform beam.
6. M. I. Qaisi 1997 *Journal of Sound and Vibration* **199**, 587–594. A power series solution for the nonlinear vibration of beams.
7. M. I. Qaisi 1998 *Journal of Sound and Vibration* **209**, 561–569. Nonlinear normal modes of a continuous systems.
8. M. Ghanbari and J. F. Dunne 1998 *Journal of Sound and Vibration* **215**, 343–379. An experimentally verified nonlinear damping model for large amplitude random vibration of a clamped–clamped beam.
9. R. M. Rosenberg 1966 *Advances in Applied Mechanics* **9**, 155–242. On nonlinear vibrations of systems with many degrees of freedom.
10. W. Szemplinska-Stupnicka 1990 *The Behavior of Nonlinear Vibrating Systems*. Vol. II. London: Kluwer Academic Publishers.
11. S. W. Shaw and C. Pierre 1993 *Journal of Sound and Vibration* **164**, 85–124. Normal modes for nonlinear vibratory systems.
12. S. W. Shaw and C. Pierre 1994 *Journal of Sound and Vibration* **169**, 319–347. Normal modes of vibration for nonlinear continuous systems.
13. A. H. Nayfeh, C. Chin and S. A. Nayfeh 1995 *Journal of Vibration and Acoustics* **116**, 477–481. Nonlinear normal modes of a cantilever beam.
14. H. Nayfeh and S. A. Nayfeh 1994 *Journal of Vibration and Acoustics* **116**, 129–136. On nonlinear modes of continuous systems.
15. S. Woinowsky-Krieger 1950 *Journal of Applied Mechanics* **17**, 35–36. The effects of axial force on the vibration of hinged bars.
16. N. Boivin, C. Pierre and S. W. Shaw 1995 *Nonlinear Dynamics* **8**, 315–346. Nonlinear normal modes, invariance, and modal dynamics approximations of nonlinear systems.
17. C. S. Hsu 1960 *Quarterly Journal of Applied Mathematics* **17**, 393–407. On the application of elliptic functions in nonlinear forced oscillations.
18. J. J. Stoker 1950 *Nonlinear vibrations*. Interscience Publisher, New York, U.S.A.
19. L. Azrar, R. Benamar and R. G. White 1999 *Journal of Sound and Vibration* **224**, 183–207. A semi-analytical approach to the nonlinear dynamic response problem of s–s and c–c beams at large vibration amplitudes part I: general theory and application to the single mode approach to free and forced vibration analysis.
20. A. H. Nayfeh 1981 *Introduction to Perturbation Techniques* New York: Wiley.
21. G. Chakraborty, A. K. Mallik and H. Hatwal 1998 *Journal of Sound and Vibration* **210**, 19–36. Normal modes and near-resonance response of beams with nonlinear effects.